

Article

Operating Parameters Optimization for the Production of Liposomes Loaded with Antibodies Using a Supercritical Fluid-Assisted Process

Pier Francesco Ferrari ^{1,2}, Paolo Trucillo ³, Giulia De Negri Atanasio ¹, Chiara Bufalini ¹, Roberta Campardelli ^{1,2,*}, Patrizia Perego ^{1,2}, Domenico Palombo ^{2,4,5} and Ernesto Reverchon ⁶

- ¹ Department of Civil, Chemical and Environmental Engineering, University of Genoa, via Opera Pia, 15, 16145 Genoa, Italy
- ² Research Center for Biologically Inspired Engineering in Vascular Medicine and Longevity, University of Genoa, via Montallegro, 1, 16145 Genoa, Italy
- ³ Department of Chemical, Materials and Industrial Production Engineering, University of Naples Federico II, Piazzale Vincenzo Tecchio, 80, 80125 Naples, Italy
- ⁴ Department of Surgical and Integrated Diagnostic Sciences, University of Genoa, viale Benedetto XV, 6, 16132 Genoa, Italy
- ⁵ Vascular and Endovascular Surgery Unit, IRCCS Ospedale Policlinico San Martino, Largo Rosanna Benzi, 10, 16132 Genoa, Italy
- ⁶ Department of Industrial Engineering, University of Salerno, via Giovanni Paolo II, 132, 84084 Fisciano, Italy
- * Correspondence: roberta.campardelli@unige.it

Abstract: Encapsulation of antibodies represents a significant advance to protect and deliver these therapeutics in a controlled manner, increasing the stability requested to cover the temporal gap between particle production and their administration. Furthermore, using encapsulation, extracellular, cell surface, and intracellular targets can be reached. This work examines the feasibility of encapsulating mouse IgG isotype control antibodies within phosphatidylcholine-based liposomes using a supercritical fluid-based process called SuperLip (Supercritical-assisted Liposome formation). This process allows a continuous production of both nano- and micrometric liposomes with high encapsulation efficiency working under mild operative conditions. The effect of some operative parameters has been studied on liposome mean diameter, particle size distribution, and antibody entrapment efficiency, comparing these data with those collected working with liposomes obtained by the thin-layer hydration technique. In particular, the effect of water flow rate and of the antibody loading were studied. Antibody-loaded liposomes with mean diameters in the range between 205 and 501 nm have been obtained by using a supercritical fluid-assisted process. High entrapment efficiencies up to 94% have been calculated.

Keywords: antibody-based therapy; supercritical fluids; drug delivery; liposomes



Citation: Ferrari, P.F.; Trucillo, P.; De Negri Atanasio, G.; Bufalini, C.; Campardelli, R.; Perego, P.; Palombo, D.; Reverchon, E. Operating Parameters Optimization for the Production of Liposomes Loaded with Antibodies Using a Supercritical Fluid-Assisted Process. *Processes* **2023**, *11*, 663. <https://doi.org/10.3390/pr11030663>

Academic Editor: Antoni Sanchez

Received: 30 December 2022

Revised: 1 February 2023

Accepted: 4 February 2023

Published: 22 February 2023



Copyright: © 2023 by the authors. Licensee MDPI, Basel, Switzerland. This article is an open access article distributed under the terms and conditions of the Creative Commons Attribution (CC BY) license (<https://creativecommons.org/licenses/by/4.0/>).

1. Introduction

The new century challenge in the treatment of chronic-degenerative diseases is represented by the possibility of having a pharmacological approach characterized by the use of nanosystems with good compliance [1], good pharmacokinetics [2], and reduced side-effects in patients [3]. Drug delivery systems offer the possibility to physically transport therapeutics exactly where they are needed [4,5]. By this approach, a reduced amount of drugs has to be administered, a longer temporal gap between repeated administrations has to be planned, and a low non-specific accumulation in organs has to be taken into account.

Next to the possibility of having a selective blockage of cellular molecules at the pathological site, the use of antibodies (Abs) [6] or inhibitors [7] has become more and more frequent. Ab-based therapy has introduced the possibility of selectively targeting molecules expressed by pathological cells, inducing their neutralization through different actions of our immune

system [8]. These therapeutic strategies have been used for many years in several protocols for cancers, rheumatoid arthritis, Crohn's disease, asthma, systemic lupus erythematosus, psoriasis, and prophylaxis of acute organ rejection, i.e., in renal transplantation [9].

The possibility to combine the selective properties of Abs with the advantages of drug delivery systems opens to the conceptualization of a new generation of Ab-based therapies. Among these strategies, current research is focusing the attention on Ab conjugation with drugs [10,11], Ab immobilization on particle surface [12–15], and Ab encapsulation in different drug delivery systems [16]. The conjugation of drugs with monoclonal antibodies (mAb) allows the carrying of cytotoxic molecules at well-defined pathological regions. Starting from the approval by the US Food and Drug Administration of Mylotarg[®] (gemtuzumab ozogamicin), Ab-drug conjugates have been commercialized and 100 candidates are now involved in clinical studies [17]. Furthermore, in order to impart to nanosystems a targeting capability, Abs are usually immobilized on their surface. Ab immobilization could be obtained through different methods, i.e., maleimide-thiol coupling, sulfhydryl chemistry, and amide bond [18]. As a result, Ab-engineered liposomes could be prepared by Ab physical adsorption, covalent attachment, and via adaptor biomolecules [19]. During the last decades, different drug delivery systems have been described, i.e., lipid-based nanosystems [20], polymeric nanoparticles [21], nanotubes [22], nanodiamonds [23], and nanofibers [24]. Among them, liposomes are vesicles made of lipids, such as phosphatidylcholine (PC), that could be produced by different techniques, i.e., the Bangham method, detergent depletion method, ethanol/ether injection method, reverse phase evaporation method, emulsion-based method, freeze-drying of monophasic solutions, microfluidic channel method, sonication, and supercritical fluid-assisted technologies [25,26]. It has been demonstrated that liposomes are biocompatible with different cell lines [27,28] and hemocompatible in a good range of concentrations [29]. Furthermore, some of their production processes can be easily scaled up [30,31]. Nowadays, different drugs are encapsulated in liposomes and approved in the pharmaceutical market, i.e., liposome-based formulations for amphotericin B, doxorubicin, morphine sulfate, verteporfin, and cytarabine [32]. Taking into account all these advantages, nanoliposomes are considered as a good choice for the encapsulation of therapeutic agents, such as Abs.

Liposome production methods are generally based on the formation of a lipid bilayer followed by its subsequent hydration that leads to their production, for example, by the Bangham method. However, these procedures are characterized by a difficult control of liposome size distribution, by the batch process layout, and by a low encapsulation efficiency (EE), with a considerable loss of the active compounds [33]. Conversely, the great advantage of the Supercritical-assisted Liposome formation (SuperLip) process is the capability to produce liposomes with a good control of size distribution, both in the nano- and micrometric range of dimensions and with a high EE, operating in a continuous mode. Indeed, in the SuperLip process water droplets are generated at first and then a lipid layer is formed around them. For this reason, a good control of dimensions and high EE values can be achieved by optimizing the water droplets formation process [34]. SuperLip has already been successfully exploited for the production of liposomes to be employed in the pharmaceutical and biomedical fields [35,36]. In particular, considering these fields of application, the advantages of this process are particularly relevant because the mild operative conditions allow to preserve the structure and the functionality of drugs and high EE values are necessary to avoid economic loss related to expensive therapeutic molecules. Furthermore, liposomes produced by using supercritical fluids are characterized by good pharmacokinetic properties that could be modulated depending on the different parameters used during the production process. In vivo tests have demonstrated the feasibility of their application in drug delivery protocols [37].

Despite the recognized advantages of supercritical fluid-assisted processes in the pharmaceutical field, the encapsulation of Abs using this approach deserves experimental studies because of the lack of scientific results [38]. Good results have been already reported for the encapsulation of proteins and peptides [39,40], representing a good basis for Ab encapsulation.

For these reasons, in this work, a feasibility study of encapsulation of mouse IgG isotype control Ab within PC-based liposomes has been performed using the SuperLip process. The different effects of process variables have been studied, such as Ab-to-lipid mass ratio (Ab/Lipids) and water flow rate (WFR). The thin-layer hydration method combined with ultrasounds in the post-processing step has been used to produce liposomes for comparison purposes.

2. Materials and Methods

2.1. Materials

Mouse IgG isotype control antibody (Ab) was purchased from Life Technologies (Carlsbad, CA, USA). For the determination of entrapment efficiency (EE), QuantumProtein bicinchoninic acid protein assay kit (BCA) (Euroclone, Pero, Italy) or Bradford reagent (SERVA Electrophoresis GmbH, Heidelberg, Germany) was used.

L- α -phosphatidylcholine (PC) from egg yolk (about 60% purity) was purchased from Sigma-Aldrich (St. Louis, MO, USA) and used as a source of phospholipids. Absolute ethanol (99.8% purity) was obtained from Carlo Erba (Milan, Italy), while carbon dioxide (>99.7% purity) was purchased from Morlando Group (Naples, Italy).

2.2. Preparation of Ab-Loaded Liposomes

SuperLip (Supercritical-assisted Liposome formation) apparatus is represented in Figure 1. It consists of a saturator, a precipitation vessel, and a storage vessel. Supercritical CO₂ is delivered to the saturator, where it is mixed with the lipid-based ethanol solution. In detail, 50, 100, or 200 mg of PC were dissolved in 100 mL of ethanol by stirring at room temperature (25 ± 2 °C) at 300 rpm for 20 min. In the saturator, an expanded liquid is formed due to the intimate mixing. The expanded liquid (i.e., a liquid that contains dissolved gas at high pressure) is then delivered to the precipitation vessel. In this last part of the plant, the formation of the liposomes occurs. In the same vessel, a nozzle (internal diameter of 80 μ m) is placed for the atomization of the water solution, in which the therapeutic molecules, i.e., Abs, are previously dispersed. After precipitation inside the formation vessel, water droplets are covered by a double lipid layer and the formed liposomes are collected at the bottom of the plant in the storage vessel.

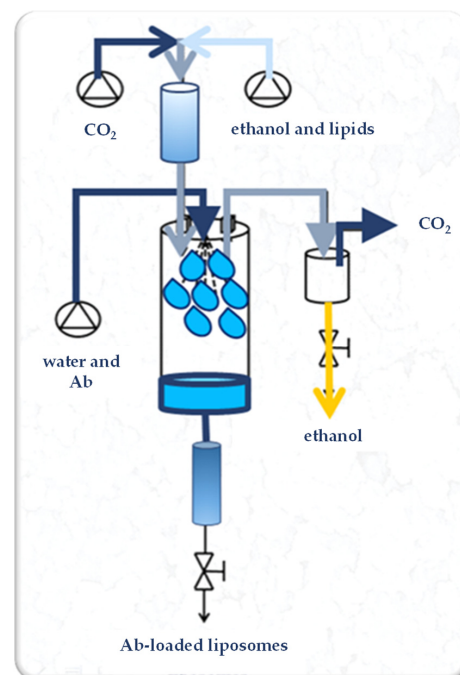


Figure 1. Experimental set-up of the SuperLip process. Ab: antibody.

Operative parameters adopted for this study were selected from a previous operative parameter optimization study [41]. In detail, the pressure was equal to 100 bar, the temperature was set at 40 °C, the lipid solution flow rate was 3.5 mL/min, the gas-to-liquid ratio (G/L) was 2.4 (*w/w*), the water solution flow rate (WFR) was in the range from 1 to 10 mL/min, and the Ab loading was from 0 to 12% (*w/w*) in respect to lipid content (Table 1).

Table 1. Operative parameters used for the production of loaded liposomes by the SuperLip apparatus. G/L: gas-to-liquid ratio, WFR: water solution flow rate, Ab/Lipids: antibody-to-lipid mass ratio.

Operative Parameter	Value
pressure	100 bar
temperature	40 °C
lipid solution flow rate	3.5 mL/min
G/L	2.4 (<i>w/w</i>)
WFR	1 or 10 mL/min
Ab/Lipids	0–12% (<i>w/w</i>)

Liposomes were also prepared by the thin-layer hydration method combined with ultrasounds. Briefly, 50, 100, or 200 mg of PC were mixed with 100 mL of ethanol until its complete dissolution. Then, using a rotary evaporator (model Laborota 4000, Heidolph Instruments GmbH & Co. KG, Schwabach, Germany), the ethanol was completely removed. The obtained lipid film was rehydrated with 20 mL of deionized water for empty liposomes or with the same amount of water containing Ab for loaded liposomes. The water solution presented different concentrations of Ab as a function of the desired Ab-to-lipid mass ratio (Ab/Lipids) and was produced starting from an Ab stock solution at 2.5 mg/mL. After water addition, the samples were left under agitation at 300 rpm for 3 h. Then, they were homogenized using a Vibra-Cell™ ultrasonic liquid processor (Sonics & Materials, Inc., Newtown, CT, USA) with a 20 kHz probe at 70% amplitude in a pulsed mode (30 s on and 30 s off) for 2 min. At the end of the production process, the obtained liposomes were centrifuged at $12,984 \times g$ for 30 min at 4 °C. The obtained supernatants were analyzed for the detection of non-encapsulated Ab [42].

2.3. Liposome Characterization

2.3.1. Particle Size

In order to measure the liposome mean diameter (LMD) and the liposome size distribution (LSD) of the obtained vesicles, the suspensions were characterized using Dynamic Light Scattering by a Zetasizer Nano ZS (Malvern Instruments Ltd., Worcestershire, UK). The instrument worked at 25 °C and was equipped with a 5.0 mW He-Ne laser operating at 633 nm with a scattering angle of 173°. At least three measurements for each sample were performed to have a LMD \pm standard deviation (SD). Regarding LSD, it has been registered after each batch of particle preparation.

2.3.2. Scanning Electron Microscopy

The morphology of the produced liposomes was studied using a field emission scanning electron microscope (FESEM) (model LEO 1525, Carl Zeiss, Oberkochen, Germany). For this analysis, a drop of each preparation was deposited over a glass slide and kept at room temperature until complete evaporation of water. Before FESEM analysis, samples were sputtered with gold in the presence of argon, obtaining a thickness of 250 Å, by an Agar Scientific device (model B7341, Stansted, UK). At least three different images for each sample were acquired.

2.3.3. Entrapment Efficiency

The EE was calculated by an indirect method. The amount of encapsulated Ab was calculated after the collection of the supernatants. Liposomes, after their preparation,

were centrifuged at $12,984 \times g$ for 30 min at 4°C , and the supernatants were collected and analyzed in terms of Ab content. EE was calculated according to Equation (1):

$$\text{EE (\%)} = \frac{\text{amount of initial Ab} - \text{amount of free Ab}}{\text{amount of initial Ab}} \times 100 \quad (1)$$

The total amount of initial Ab is referred to as the Ab initially fed during the preparation procedures, while free Ab represents the protein found in the supernatants after the centrifugation step, i.e., the non-encapsulated ones. The Ab concentration was measured by BCA or by Bradford reagent following the manufacturer's instructions and the absorbance of the samples was read at 562 or 595 nm, respectively, using a microplate reader (Tecan Spark[®] 20M, Tecan, Männedorf, Switzerland). This analysis was performed in triplicate.

2.3.4. Statistical Analysis

All the experiments were done in triplicate and the results are expressed as mean values \pm SD. Statistical analysis was performed by one-way analysis of variance (ANOVA), following Tukey's HSD (honestly significant difference) post-hoc multiple comparison test using Statistica version 8.0 software (StatSoft, Tulsa, OK, USA).

3. Results and Discussion

A first set of experiments was performed at the operative conditions of 100 bar, 40°C , lipid solution flow rate set at 3.5 mL/min, gas-to-liquid ratio (G/L) equal to 2.4 (*w/w*), water solution flow rate (WFR) at 1 mL/min, and varying the Ab-to-lipid mass ratio (Ab/Lipids) from 0.625 to 2.5% (*w/w*), obtained using different concentration of PC dissolved in the ethanolic solution, respectively from 0.5 to 2 mg/mL. Ab was used at 2.5 mg/mL. Experiments for the production of empty liposomes (A0), as a control, were also performed.

Results in terms of LMD, polydispersity index (PDI), ζ -potential, and EE are reported in Table 2.

Table 2. SuperLip experimental operative conditions and liposome characterization parameters. Different letters (a, b, and c) in the LMD, ζ -potential, and EE column refer to statistically significant differences among the different samples of each column ($p < 0.05$) by ANOVA with Tukey's HSD post-hoc multiple comparison test. WFR: water flow rate, Ab/Lipids: antibody-to-lipid mass ratio, LMD: liposome mean diameter, SD: standard deviation, PDI: polydispersity index, EE: encapsulation efficiency.

Test	WFR (mL/min)	Ab/Lipids (% <i>w/w</i>)	LMD \pm SD (nm)	PDI	ζ -Potential (mV)	EE \pm SD (%)
A0	1	0	169.61 \pm 4.11 ^a	0.39 \pm 0.01	−2.91 \pm 0.47 ^a	—
A1	1	0.625	345.95 \pm 2.93 ^b	0.33 \pm 0.05	−7.53 \pm 0.54 ^b	53.70 \pm 5.59 ^a
A2	1	1.25	501.03 \pm 36.70 ^c	0.56 \pm 0.22	−3.84 \pm 0.34 ^c	62.54 \pm 12.15 ^a
A3	1	2.50	464.55 \pm 128.50 ^{b,c}	0.68 \pm 0.04	−5.63 \pm 2.98 ^{a,b,c}	35.83 \pm 4.93 ^b
A4	10	0.625	144.65 \pm 1.73 ^a	0.25 \pm 0.02	−12.53 \pm 0.38 ^a	93.62 \pm 1.74 ^a
A5	10	1.25	319.90 \pm 25.00 ^b	0.52 \pm 0.11	−38.28 \pm 3.85 ^b	28.06 \pm 0.52 ^b
A6	10	2.50	205.00 \pm 2.34 ^c	0.25 \pm 0.02	−14.30 \pm 1.28 ^a	48.03 \pm 9.33 ^c
A7	10	1	369.58 \pm 149.78 ^a	0.58 \pm 0.44	−7.39 \pm 0.53 ^a	65.91 \pm 3.13 ^a
A8	10	4	366.00 \pm 4.50 ^a	0.25 \pm 0.02	−7.49 \pm 1.22 ^a	82.36 \pm 12.30 ^b
A9	10	12	317.07 \pm 6.73 ^a	0.27 \pm 0.03	−15.20 \pm 1.53 ^b	80.34 \pm 12.63 ^{a,b}

Considering the first experimental set (A1, A2, and A3), LMD augmented with the increase of the Ab/Lipids up to 501.03 \pm 36.70 nm. Indeed, empty liposomes were characterized by a LMD equal to 169.61 \pm 4.11 nm. This effect was probably due to the presence of the drug in the inner aqueous core, whose increase can produce a larger internal volume of the entrapped phase. The obtained liposomes possessed a negative ζ -potential value for

each preparation. ζ -potential values ranged between -2.91 ± 0.47 (empty liposomes) and -7.53 ± 0.54 mV. This characteristic could be considered an advantage for constructs that will follow the injection route. In fact, negative particles do not significantly adsorb blood protein and can potentially be recognized by macrophages, one of the potential targets in inflammatory-based diseases in which Ab-based therapy could have a pivotal role [43]. In the first experimental set, EE values ranged between 35.83 ± 4.93 and $62.54 \pm 12.15\%$.

Figure 2 shows LSD, highlighting that liposomes with submicrometer diameters were obtained in all the experiments. Examples of FESEM images of the prepared liposomes are reported in Figure 3 where empty liposomes (Figure 3A) and Ab-loaded ones (Figure 3B) are compared. Liposomes appeared to be characterized by a spherical shape and were uniform [41].

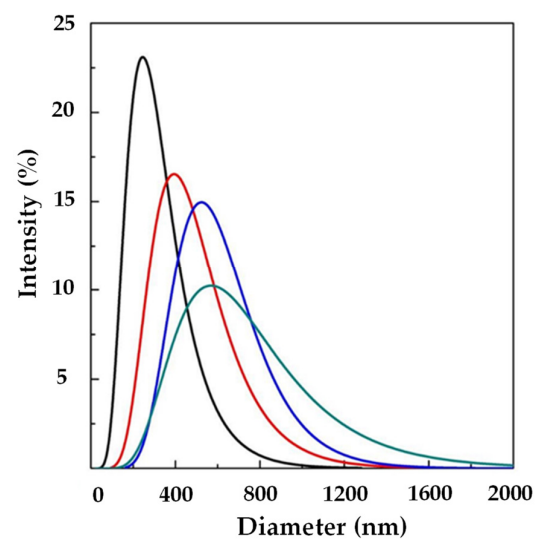


Figure 2. LSD by intensity at different Ab/Lipids in the presence of WFR fixed at 1 mL/min: (—) 0, (—) 0.625, (—) 1.25, and (—) 2.50% (*w/w*). LSD: liposome size distribution Ab/Lipids: antibody-to-lipid mass ratio, WFR: water flow rate.

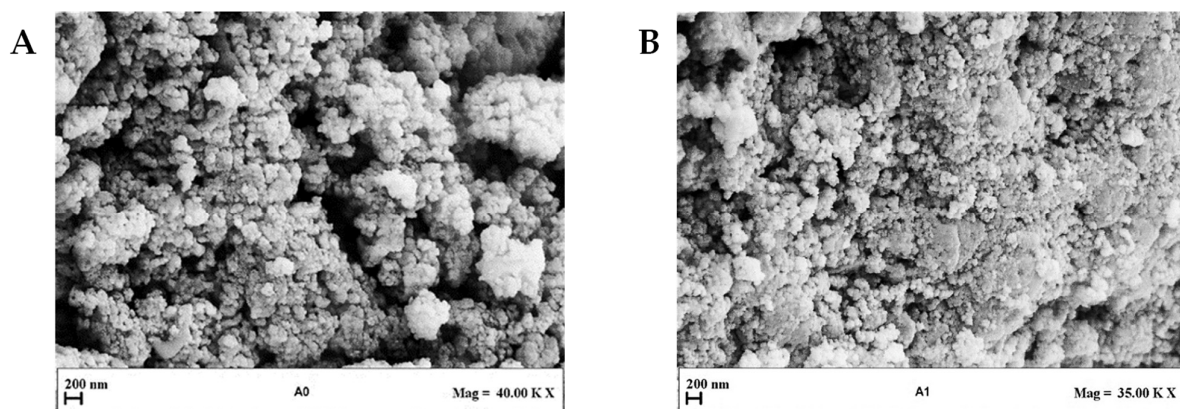


Figure 3. Representative FESEM images of liposomes produced at different Ab/Lipids and at a fixed WFR of 1 mL/min: (A) Sample with Ab/Lipids equal to 0% (*w/w*) and (B) Sample with Ab/Lipids equal to 0.625% (*w/w*). FESEM: field emission scanning electron microscope, Ab/Lipids: antibody-to-lipid mass ratio, WFR: water flow rate.

In order to try to improve the EE, another set of experiments (A4, A5, and A6) was performed using SuperLip at a higher WFR (10 mL/min). The same Ab/Lipids was fixed for comparison purposes. Smaller liposomes were produced in this case, with a LMD in the range between 144.65 ± 1.73 and 319.90 ± 25.00 nm, as shown in Table 2. Also in this case,

by augmenting the Ab/Lipids, an increase in LMD was observed (Figure 4). However, a good control of LSD was always guaranteed.

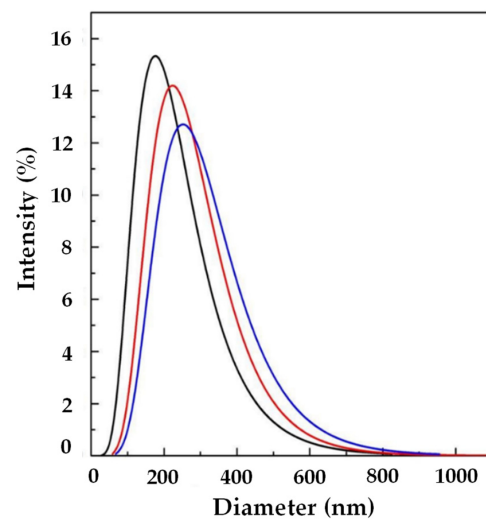


Figure 4. LSD by intensity at different Ab/Lipids in the presence of WFR fixed at 10 mL/min: (—) 0.625, (—) 1.25, and (—) 2.50% (*w/w*). LSD: liposome size distribution, Ab/Lipids: antibody-to-lipid mass ratio, WFR: water flow rate.

A representative FESEM image of liposomes obtained in this set of experiments is reported in Figure 5. It can be observed that the liposomes showed spherical morphology. The EE increased to $93.62 \pm 1.74\%$ in the case of Ab/Lipids equal to 0.625% (*w/w*), but it was drastically reduced as the theoretical Ab loading increased, reaching a minimum value of $28.06 \pm 0.52\%$. In general, the increase in WFR did not produce a substantial improvement in the EE, but it was considered a better operative condition since it allowed an improvement in LSD.

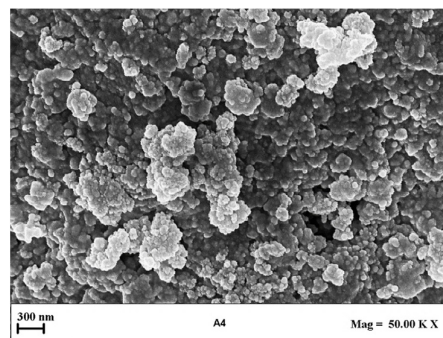


Figure 5. Representative FESEM image of liposomes produced at Ab/Lipids equal to 0.625% (*w/w*) and at a fixed WFR of 10 mL/min. FESEM: field emission scanning electron microscope, Ab/Lipids: antibody-to-lipid mass ratio, WFR: water flow rate.

Another set of experiments (A7, A8, and A9) was performed at 10 mL/min of WFR, changing the Ab/Lipids with the aim of increasing the EE. In particular, Ab/Lipids equal to 1, 4, or 12% (*w/w*) were tested. Taking into account the reported results in Table 2 and in Figure 6, it can be observed that uniform liposomes were produced in terms of LMD that was in the range between 317.07 ± 6.73 and 369.58 ± 149.78 nm. LSD was wide as a consequence of the increase in the active molecule loading. Furthermore, these formulations showed a good ζ -potential.

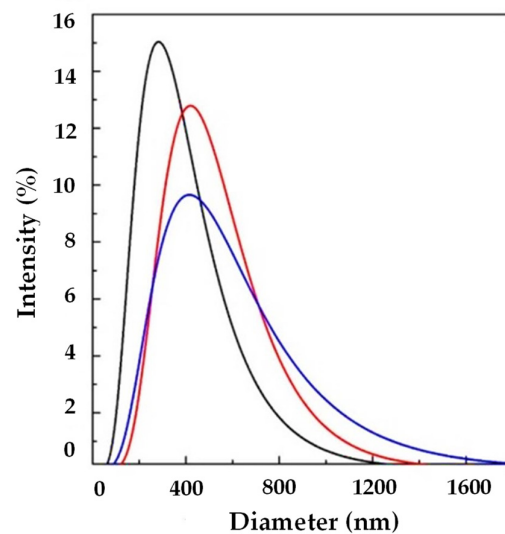


Figure 6. LSD by intensity at different Ab/Lipids in the presence of WFR fixed at 10 mL/min: (—) 1, (—) 4, and (—) 12% (*w/w*). LSD: liposome size distribution, Ab/Lipids: antibody-to-lipid mass ratio, WFR: water flow rate.

An increase in EE was obtained from 65.91 ± 3.13 to $82.36 \pm 12.30\%$. At these operative conditions, it was possible to obtain submicrometer-sized vesicles with a good EE.

For comparison purposes, liposomes with the same Ab/Lipids were produced by the thin-layer hydration method combined with ultrasounds to have a diameter reduction. This technique is known to be one of the most efficient in producing submicrometer-sized liposomes. The more conventional techniques are discontinuous and, therefore, from a practical point of view, will produce batch-to-batch differences that have to be avoided for pharmaceutical applications. The Ab/Lipids was varied from 0 to 5% (*w/w*), using different amounts of PC (50, 100, or 200 mg) dissolved in ethanol. Experiments for the production of empty liposomes (B0), as a control, were also performed.

Results in terms of LMD, PDI, ζ -potential, and EE are reported in Table 3.

Table 3. Thin-layer hydration experimental operative conditions and liposome characterization parameters. Different letters (a, b, and c) in the LMD, ζ -potential, and EE column refer to statistically significant differences among the different samples of each column ($p < 0.05$) by ANOVA with Tukey's HSD post-hoc multiple comparison test. Ab/Lipids: antibody-to-lipid mass ratio, LMD: liposome mean diameter, SD: standard deviation, PDI: polydispersity index, EE: encapsulation efficiency.

Test	Ab/Lipids (% <i>w/w</i>)	LMD \pm SD (nm)	PDI	ζ -Potential (mV)	EE \pm SD (%)
B0	0	483.63 ± 12.33 ^a	0.60 ± 0.04	-29.70 ± 1.42 ^a	—
B1	1.25	575.87 ± 50.31 ^b	0.72 ± 0.16	-24.30 ± 0.82 ^b	79.10 ± 1.01 ^a
B2	2.5	284.67 ± 4.74 ^c	0.44 ± 0.01	-28.43 ± 2.07 ^a	64.12 ± 0.63 ^b
B3	5.0	600.53 ± 20.30 ^b	0.56 ± 0.06	-20.67 ± 0.86 ^b	61.80 ± 0.98 ^c

The first experimental set of liposomes obtained by the thin-layer hydration method (B1, B2, and B3) were characterized by submicrometer dimensions with a diameter in the range between 284.67 ± 4.74 and 600.53 ± 20.30 nm, mainly due to ultrasounds used in the post-processing step. Only in the case of Ab/Lipids equal to 2.5% (*w/w*) there was a reduction in the observed diameter in comparison also with empty liposomes. The values of ζ -potential of loaded liposomes were in the range between -20.67 ± 0.86 and -28.43 ± 2.07 mV. These values indicated high repulsion forces among the particles ensuring their stability.

Comparing these liposomes with those obtained by using SuperLip, it was possible to observe that liposomes produced with the conventional method showed a larger PDI and, therefore, a broader LSD. This was due to the fact that SuperLip provided the atomization of the aqueous phase and therefore there was a more efficient dimensional control over the diameter of the produced liposomes.

The EE reached a maximum value of $79.10 \pm 1.01\%$, comparable with the EE percentages obtained using the supercritical fluid-assisted method, but liposomes produced by the SuperLip method showed better control of LSD. Furthermore, the SuperLip process allowed us to work in a continuous mode with higher productivity.

To compare the SuperLip technique with the conventional hydration method, followed by ultrasounds, another set of liposomes (B4, B5, and B6) with the same Ab/Lipids were produced. The Ab/Lipids was varied from 1 to 12% (*w/w*), changing the volume of Ab solution and fixing the amount of PC at 50 mg. Results are reported in Table 4 in terms of LMD, PDI, and EE.

Table 4. Thin-layer hydration method experimental operative conditions and liposome characterization parameters. Different letters (a, b, and c) in the LMD and EE column refer to statistically significant differences among the different samples of each column ($p < 0.05$) by ANOVA with Tukey's HSD post-hoc multiple comparison test. Ab/Lipids: antibody-to-lipid mass ratio, LMD: liposome mean diameter, SD: standard deviation, PDI: polydispersity index, EE: encapsulation efficiency.

Test	Ab/Lipids (% <i>, w/w</i>)	LMD \pm SD (nm)	PDI	EE \pm SD (%)
B4	1	367.27 ± 6.37^a	0.57 ± 0.01	87.39 ± 8.52^a
B5	4	714.27 ± 9.64^b	0.55 ± 0.18	69.81 ± 4.35^a
B6	12	842.17 ± 23.96^c	0.31 ± 0.17	88.01 ± 3.60^a

Using this technique, submicron-sized liposomes were produced with an average diameter in the range between 367.27 ± 6.37 and 842.17 ± 23.96 nm. The size increased with the increase of the Ab/Lipids. Comparing the liposomes listed in Table 4 with the loaded liposomes produced by SuperLip (Figure 7), it can be seen that, fixed the Ab/Lipids value, the supercritical CO₂ permitted to obtain smaller sizes (Figure 7A).

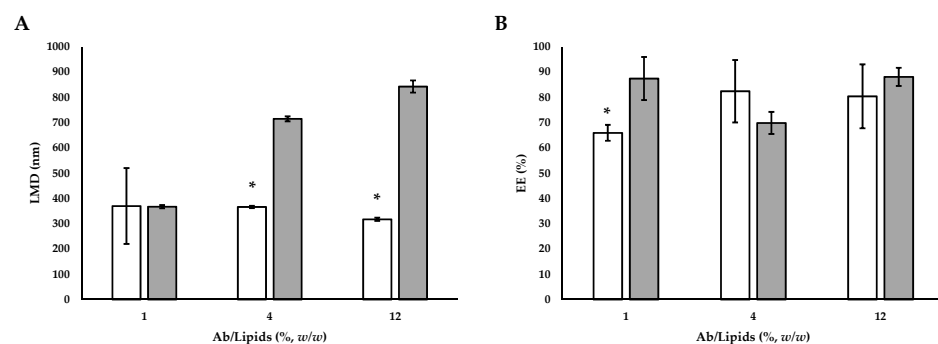


Figure 7. (A) Comparative analysis of LMD and (B) EE between Ab-loaded liposomes prepared by SuperLip process and those prepared by thin-layer hydration method. The symbol (*) refers to statistically significant differences among results ($p < 0.05$, ANOVA with Tukey's HSD post-hoc multiple comparison test). □ SuperLip process and ■ thin-layer hydration method. LMD: liposome mean diameter, Ab/Lipids: antibody-to-lipid mass ratio, EE: entrapment efficiency.

The EE values for liposomes produced using the thin-layer hydration method combined with ultrasounds ranged between 69.81 ± 4.35 and $88.01 \pm 3.60\%$. From the obtained results, EE was not dependent on Ab loading (Table 4). Therefore, it was highlighted that loading more active ingredients for the same lipid amount did not lead to an improvement

in EE. On the contrary, working with the SuperLip process, the EE values were higher. This behavior was related to the different ways of the liposome formation. In the SuperLip process, the atomization of the aqueous solution with Ab and the subsequent coating with the lipid bilayer allowed to maximize the EE. Therefore, augmenting the loading also partially increased the effective encapsulation and allowed to limit the loss of Ab in the external bulk of the suspension. This fact was particularly advantageous for Abs with high costs. However, no differences in terms of EE percentage were noticed between SuperLip and the thin-layer hydration method working at the highest values of Ab/Lipids (Figure 7B).

Therefore, the SuperLip process is more performing in terms of dimensional control and EE. Using a higher flow rate of Ab aqueous solution and working with Ab/Lipids equal to 0.625% (*w/w*), there was an increase in the EE up to values around 94%, guaranteeing at the same time a good dimensional control.

4. Conclusions

A supercritical fluid-assisted process has been used in this work for the production of liposomes loaded with mouse IgG control antibody (Ab). In order to guarantee a high protection of the liposome content, the phospholipid membrane was designed after a deep study of the operating parameters. In order to get better bioavailability, liposomes were produced at the submicrometer level after optimizing process conditions. A comparison with a conventional method of production was provided in order to underline the lack of protection and bioavailability of liposomes of larger dimensions with lower encapsulation efficiencies (EE). The advantages introduced by the supercritical fluid-assisted process resulted in a significantly increased EE compared to the conventional process, which is regulated by room temperature and atmospheric pressure with non-predictable aggregative phenomena. The EE values up to 93.64%, obtained by using SuperLip, resulted in the possibility of preserving a large amount of Abs making them available to target cells. The potential of the process guarantees a significantly reduced cost for raw materials, which is particularly dependent on the cost of the encapsulated Ab in this case.

The optimized conditions for the production of lipid vesicles loaded with Abs open the scenario to the encapsulation of DNA or to obtain vaccines, according to the good manufacturing practice requirements. Future perspectives will consist in the development of liposomes loaded with Abs in sterile conditions, activating a further experimental campaign for the *in vitro* and *in vivo* applications with human cells and model animals, respectively. Before doing that, it will be crucial to bypass the limits of the formulations presented in this work trying to increase EE, lowering polydispersity index, and characterizing the Ab functionality after the encapsulation process.

Author Contributions: Conceptualization, P.F.F., P.T., R.C., P.P., D.P. and E.R.; methodology, P.F.F., P.T., G.D.N.A., C.B. and R.C.; investigation, P.F.F., P.T., G.D.N.A., C.B. and R.C.; resources, R.C., P.P., D.P. and E.R.; data curation, P.F.F., P.T., G.D.N.A., C.B. and R.C.; writing—original draft preparation, P.F.F., P.T., G.D.N.A., C.B. and R.C.; writing—review and editing, P.F.F., P.T., R.C., P.P., D.P. and E.R.; supervision, P.F.F., R.C., P.P., D.P. and E.R.; project administration, P.F.F., P.T., R.C., P.P., D.P. and E.R.; funding acquisition, R.C., P.P., D.P. and E.R. All authors have read and agreed to the published version of the manuscript.

Funding: This work was financed by “Fondi di Ricerca di Ateneo” (100010-2018-DP-FRA_001) and “Curiosity-driven project 2020” (100024-2020-RC-CURIOSITY_001), University of Genoa.

Data Availability Statement: The data presented in this study are available on request from the corresponding author.

Conflicts of Interest: The authors declare no conflict of interest.

References

1. Anselmo, A.C.; Mitragotri, S. An overview of clinical and commercial impact of drug delivery systems. *J. Control. Release* **2014**, *190*, 15–28.
2. Chen, R.; Wang, T.; Song, J.; Pu, D.; He, D.; Li, J.; Yang, J.; Li, K.; Zhong, C.; Zhang, J. Antiviral drug delivery system for enhanced bioactivity, better metabolism and pharmacokinetic characteristics. *Int. J. Nanomed.* **2021**, *16*, 4959–4984. [[CrossRef](#)] [[PubMed](#)]
3. Allen, T.M.; Cullis, P.R. Drug delivery systems: Entering the mainstream. *Science* **2004**, *303*, 1818–1822. [[CrossRef](#)] [[PubMed](#)]
4. Liu, D.; Yang, F.; Xiong, F.; Gu, N. The smart drug delivery system and its clinical potential. *Theranostics* **2016**, *6*, 1306–1323. [[CrossRef](#)] [[PubMed](#)]
5. Wang, J.; Li, Y.; Nie, G. Multifunctional biomolecule nanostructures for cancer therapy. *Nat. Rev. Mater.* **2021**, *6*, 766–783. [[CrossRef](#)]
6. Goulet, D.R.; Atkins, W.M. Considerations for the design of antibody-based therapeutics. *J. Pharm. Sci.* **2020**, *109*, 74–103. [[CrossRef](#)]
7. Manzari, M.T.; Shamay, Y.; Kiguchi, H.; Rosen, N.; Scaltriti, M.; Heller, D.A. Targeted drug delivery strategies for precision medicines. *Nat. Rev. Mater.* **2021**, *6*, 351–370. [[CrossRef](#)]
8. Weiner, G.J. Building better monoclonal antibody-based therapeutics. *Nat. Rev. Cancer* **2015**, *15*, 361–370. [[CrossRef](#)]
9. Samaranyake, H.; Wirth, T.; Schenkwein, D.; Rätty, J.K.; Ylä-Herttua, S. Challenges in monoclonal antibody-based therapies. *Ann. Med.* **2009**, *41*, 322–331. [[CrossRef](#)]
10. Beck, A.; Goetsch, L.; Dumontet, C.; Corvaia, N. Strategies and challenges for the next generation of antibody-drug conjugates. *Nat. Rev. Drug Discov.* **2017**, *16*, 315–337. [[CrossRef](#)]
11. Joubert, N.; Beck, A.; Dumontet, C.; Denevault-Sabourin, C. Antibody-drug conjugates: The last decade. *Pharmaceuticals* **2020**, *13*, 245. [[CrossRef](#)] [[PubMed](#)]
12. Kocbek, P.; Obermajer, N.; Cegnar, M.; Kos, J.; Kristl, J. Targeting cancer cells using PLGA nanoparticles surface modified with monoclonal antibody. *J. Control. Release* **2007**, *120*, 18–26. [[CrossRef](#)]
13. Helmi, O.; Elshishiny, F.; Mamdouh, W. Targeted doxorubicin delivery and release within breast cancer environment using PEGylated chitosan nanoparticles labeled with monoclonal antibodies. *Int. J. Biol. Macromol.* **2021**, *184*, 325–338. [[CrossRef](#)] [[PubMed](#)]
14. Shimizu, K.; Takeuchi, Y.; Otsuka, K.; Mori, T.; Narita, Y.; Takasugi, S.; Magata, Y.; Matsumura, Y.; Oku, N. Development of tissue factor-targeted liposomes for effective drug delivery to stroma-rich tumors. *J. Control. Release* **2020**, *323*, 519–529. [[CrossRef](#)] [[PubMed](#)]
15. Misra, S.K.; Pathak, K. Functionalized liposomes: A nanovesicular system. In *Systems of Nanovesicular Drug Delivery*; Academic Press: Cambridge, MA, USA, 2022; pp. 83–101.
16. De Negri Atanasio, G.; Ferrari, P.F.; Baião, A.; Perego, P.; Sarmento, B.; Palombo, D.; Campardelli, R. Bevacizumab encapsulation into PLGA nanoparticles functionalized with immunoglobulin-1 as an innovative delivery system for atherosclerosis. *Int. J. Biol. Macromol.* **2022**, *221*, 1618–1630. [[CrossRef](#)]
17. Fu, Z.; Li, S.; Han, S.; Shi, C.; Zhang, Y. Antibody drug conjugate: The “biological missile” for targeted cancer therapy. *Signal Transduct. Target. Ther.* **2022**, *7*, 93. [[CrossRef](#)]
18. Moulahoum, H.; Ghorbanizamani, F.; Zihnioglu, F.; Timur, S. Surface biomodification of liposomes and polymersomes for efficient targeted drug delivery. *Bioconjug. Chem.* **2021**, *32*, 1491–1502. [[CrossRef](#)]
19. Sivaram, A.J.; Wardiana, A.; Howard, C.B.; Mahler, S.M.; Thurecht, K.J. Recent advances in the generation of antibody-nanomaterial conjugates. *Adv. Healthc. Mater.* **2018**, *7*, 1700607. [[CrossRef](#)]
20. Mitchell, M.J.; Billingsley, M.M.; Haley, R.M.; Wechsler, M.E.; Peppas, N.A.; Langer, R. Engineering precision nanoparticles for drug delivery. *Nat. Rev. Drug Discov.* **2021**, *20*, 101–124. [[CrossRef](#)]
21. De Negri Atanasio, G.; Ferrari, P.F.; Campardelli, R.; Perego, P.; Palombo, D. Innovative nanotools for vascular drug delivery: The atherosclerosis case study. *J. Mater. Chem. B* **2021**, *9*, 8558–8568. [[CrossRef](#)]
22. Bianco, A.; Kostarelos, K.; Prato, M. Applications of carbon nanotubes in drug delivery. *Curr. Opin. Chem. Biol.* **2005**, *9*, 674–679. [[CrossRef](#)] [[PubMed](#)]
23. Kaur, R.; Badea, I. Nanodiamonds as novel nanomaterials for biomedical applications: Drug delivery and imaging systems. *Int. J. Nanomed.* **2013**, *8*, 203–220. [[PubMed](#)]
24. Yu, D.G.; Zhu, L.M.; White, K.; Branford-White, C. Electrospun nanofiber-based drug delivery systems. *Health* **2009**, *1*, 67–75. [[CrossRef](#)]
25. Maherani, B.; Arab-Tehrany, E.; Mozafari, M.R.; Gaiani, C.; Linder, M. Liposomes: A review of manufacturing techniques and targeting strategies. *Curr. Nanosci.* **2011**, *7*, 436–452. [[CrossRef](#)]
26. Bigazzi, W.; Penoy, N.; Evrard, B.; Piel, G. Supercritical fluid methods: An alternative to conventional methods to prepare liposomes. *Chem. Eng. J.* **2020**, *383*, 123106.
27. Homayoonfal, M.; Mousavi, S.M.; Kiani, H.; Askari, G.; Desobry, S.; Arab-Tehrany, E. Encapsulation of *Berberis vulgaris* anthocyanins into nanoliposome composed of rapeseed lecithin: A comprehensive study on physicochemical characteristics and biocompatibility. *Foods* **2021**, *10*, 492. [[CrossRef](#)]

28. Hanachi, A.; Bianchi, A.; Kahn, C.J.F.; Velot, E.; Arab-Tehrany, E.; Cakir-Kiefer, C.; Linder, M. Encapsulation of salmon peptides in marine liposomes: Physico-chemical properties, antiradical activities and biocompatibility assays. *Mar. Drugs* **2022**, *20*, 249. [[CrossRef](#)]
29. Lakkadwala, S.; dos Santos Rodrigues, B.; Sun, C.; Singh, J. Dual functionalized liposomes for efficient co-delivery of anti-cancer chemotherapeutics for the treatment of glioblastoma. *J. Control. Release* **2019**, *307*, 247–260. [[CrossRef](#)]
30. Carneiro, A.L.; Santana, M.H.A. Production of liposomes in a multitubular system useful for scaling up of processes. *Progr. Colloid Polym. Sci.* **2004**, *128*, 273–277.
31. Charcosset, C.; Juban, A.; Valour, J.-P.; Urbaniak, S.; Fessi, H. Preparation of liposomes at large scale using the ethanol injection method: Effect of scale-up and injection devices. *Chem. Eng. Res. Des.* **2015**, *94*, 508–515. [[CrossRef](#)]
32. Bozzuto, G.; Molinari, A. Liposomes as nanomedical devices. *Int. J. Nanomedicine* **2015**, *10*, 975–999. [[CrossRef](#)] [[PubMed](#)]
33. Meure, L.A.; Foster, N.R.; Dehghani, F. Conventional and dense gas techniques for the production of liposomes: A review. *AAPS PharmSciTech* **2008**, *9*, 798–809. [[CrossRef](#)] [[PubMed](#)]
34. Trucillo, P.; Campardelli, C.; Reverchon, E. Liposomes: From Bangham to supercritical fluids. *Processes* **2020**, *8*, 1022. [[CrossRef](#)]
35. Campardelli, C.; Trucillo, P.; Reverchon, E. Supercritical assisted process for the efficient production of liposomes containing antibiotics for ocular delivery. *J. CO₂ Util.* **2018**, *25*, 235–241. [[CrossRef](#)]
36. Trucillo, P.; Campardelli, C.; Reverchon, E. A versatile supercritical assisted process for the one-shot production of liposomes. *J. Supercrit. Fluids* **2019**, *146*, 136–143. [[CrossRef](#)]
37. Lim, C.-b.; Abuzar, S.M.; Karn, P.R.; Cho, W.; Park, H.J.; Cho, C.-W.; Hwang, S.-J. Preparation, characterization, and in vivo pharmacokinetic study of the supercritical fluid-processed liposomal amphotericin B. *Pharmaceutics* **2019**, *11*, 589. [[CrossRef](#)]
38. Tabertero, A.; González-Garcinuno, A.; Galán, M.A.; Martín del Valle, E.M. Survey of supercritical fluid techniques for producing drug delivery systems for a potential use in cancer therapy. *Rev. Chem. Eng.* **2016**, *32*, 507–532. [[CrossRef](#)]
39. Campardelli, R.; Espirito Santo, I.; Albuquerque, E.C.; de Melo, S.V.; Della Porta, G.; Reverchon, E. Efficient encapsulation of proteins in submicro liposomes using a supercritical fluid assisted continuous process. *J. Supercrit. Fluids* **2016**, *107*, 163–169. [[CrossRef](#)]
40. Palazzo, I.; Lamparelli, E.P.; Ciardulli, M.C.; Scala, P.; Reverchon, E.; Forsyth, N.; Maffulli, N.; Santoro, A.; Della Porta, G. Supercritical emulsion extraction fabricated PLA/PLGA micro/nano carriers for growth factor delivery: Release profiles and cyto-toxicity. *Int. J. Pharm.* **2021**, *592*, 120108. [[CrossRef](#)]
41. Trucillo, P.; Campardelli, R.; Scognamiglio, M.; Reverchon, E. Control of liposomes diameter at micrometric and nanometric level using a supercritical assisted technique. *J. CO₂ Util.* **2019**, *32*, 119–127. [[CrossRef](#)]
42. De Negri Atanasio, G.; Ferrari, P.F.; Campardelli, R.; Perego, P.; Palombo, D. Poly (lactic-co-glycolic acid) nanoparticles and nanoliposomes for protein delivery in targeted therapy: A comparative in vitro study. *Polymers* **2020**, *12*, 2566. [[CrossRef](#)] [[PubMed](#)]
43. Honary, S.; Zahir, F. Effect of zeta potential on the properties of nano-drug delivery systems - A review (Part 2). *Trop. J. Pharm. Res.* **2013**, *12*, 265–273.

Disclaimer/Publisher’s Note: The statements, opinions and data contained in all publications are solely those of the individual author(s) and contributor(s) and not of MDPI and/or the editor(s). MDPI and/or the editor(s) disclaim responsibility for any injury to people or property resulting from any ideas, methods, instructions or products referred to in the content.